

# Waves in the Summer Ice in the Winter

Atle Lohrmann  
Torstein Pedersen  
Sven Nylund  
Nortek AS  
Norway  
inquiry@nortek-as.com

Eric Siegel  
NortekUSA  
Annapolis, Maryland, USA

**Abstract**— Nortek provides a combined wave and current profiling instrument in the form of the AWAC. This variant of the traditional ADCP has managed to circumvent the classic limitations of measuring short waves in deep waters by introducing a vertical beam that directly measures the height of the water-air interface (waves) above the instrument. This same vertical beam has also demonstrated that it is capable of measuring the distance to the water-ice interface, and as a result can be used as means to estimate ice draft or ice thickness.

Measurement campaigns that have taken place in relatively shallow coastal waters (less than 50 meters) are finding themselves more often in deeper waters. These deployments are also occurring at more extreme latitudes where the presence of ice is more common. This means that common measurement requirements now include measuring ice thickness in addition to current profiles and directional wave observations.

Nortek has addressed this need of measurements in deeper waters by building upon the success of the AWAC. A 400 kHz AWAC has been developed and intended for deployment depths of 100 meters. The 400 kHz AWAC is outfitted with a temperature compensated pressure sensor and firmware with a dual functioning surface tracking measurements for ice and waves. The wave burst measurement contains detection methods for both water-air interface and water-ice interface; this means the AWAC can transition seamlessly from wave measurements in the summer to ice measurements in the winter.

Ice thickness data is presented for two AWACs deployed in the Beaufort Sea, Alaska. These data are compared to an ASL ice profiler. AWAC data was collected in a special diagnostic mode and allowed for the user to select the best water-ice interface detection method in post-processing. The results show that there is favorable agreement between the AWAC and the ASL ice profiler. This data set was useful in developing the now existing firmware used to detect the water-ice interface. These shallow water data did not illustrate errors associated with an unknown speed of sound profile – which is identified as the primary source of error for the AST distance measurement.

Additionally, wave results are presented for the 400 kHz AWAC and compared to a 600 kHz AWAC, which was deployed in the vicinity. The data show that non-directional estimates agree well, however directional estimates are complicated by the fact that the two AWACs were deployed at different locations and exposed to different wave directions due to local refraction. It is clear that another comparison test needs to be conducted with the reference instrument collocated with the 400 kHz AWAC.

**Keywords** - AWAC; ADCP; ice thickness; wave measurements

## I. INTRODUCTION

The AWAC is an established current profiling and wave measurement instrument. Current profiles employ acoustic Doppler measurements (standard for an ADCP) and wave measurements use both the near-surface Doppler velocity measurements, and a dedicated vertical, narrow beam for echo ranging. The echo ranging is commonly referred to as Acoustic Surface Tracking (AST), as it traces the surface wave profile as it passes through its field of view.

The latest development is a 400 kHz AWAC (Fig. 1), which is intended for greater deployment depths and profiling ranges. The 400 kHz AWAC is actually a dual frequency instrument, where the off vertical beams, which are used for current profile measurements, transmit at 400 kHz and the vertical beam, used for AST, transmits at 600 kHz. Despite the dual frequencies, Nortek refers to this instrument as the 400 kHz AWAC.

The vertical beam transmits at a higher frequency in order to maintain the beam's narrow opening angle (1.7 degrees). The 400 kHz AWAC can measure waves and currents over a full depth of 100 meters. The AST has demonstrated that it is also well suited for other tasks, such as ice thickness measurements.

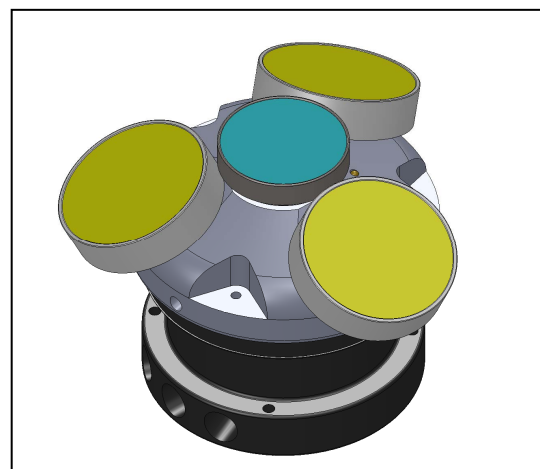


Figure 1. 400 kHz AWAC with 400 kHz off-vertical transducers (yellow) and 600 kHz center, AST transducer (blue).

Ice thickness estimates from the subsurface requires an accurate depth estimate and an accurate distance measurement (AST). In order to fulfill this requirement, the 400 kHz AWAC now has a temperature compensated pressure sensor to reduce the uncertainty in the pressure measurements. The AST measurements have been modified by including a second ranging estimate by using a different filter for the water-ice interface, which is different than that used for detecting the water-air interface. Either ice or wave processing can be performed since both estimates are reported within the same wave burst. This makes it ideal for yearlong deployments at extreme latitudes where the same measurement scheme is used for waves in the summer, ice thickness in the winter, and both during the transitional periods in the spring and fall.

One notable difference for the 400 kHz AWAC is that in order for an individual AST ping to have enough time to reach the surface and back, the sampling rate had to be reduced to 1.5 Hz. This means the AST samples at 1.5 Hz and the pressure and velocity sample at 0.75 Hz. Furthermore, the selection for the total number of samples is maintained at 512, 1024, and 2048 samples. This extends the burst length to approximately 11.25, 22.5, and 45 minutes, respectively.

## II. SUBSURFACE WAVE MEASUREMENTS

### A. Background

It is quite common to measure waves from a surface buoy. However, there are some locations that preclude this on practical grounds, as well as many other locations that present challenges to the survivability of surface buoys. Such challenges include shipping traffic, vandalism, and ice. One alternative is to measure from below the surface. The method has shown good results, however it is limited to shallow, coastal waters or to measurements of only long waves. There have been notable developments which have improved upon these earlier shortcomings; much of these improvements have occurred in the last ten years. A brief review of the developments follows.

Subsurface wave measurements were initially performed with the PUV class of instruments where pressure and wave orbital velocity were measured at the instrument's deployment depth. The method works well, but suffers from the fact that short waves attenuate with depth; as a result, PUV type of instruments are limited to coastal waters that are typically less than 10-15 meters [1].

The introduction of the ADCP improved the performance by measuring wave orbital velocities closer to the surface which are less attenuated than those further down in the water column [2]; this effectively doubled the deployments depths which were possible with PUV instruments. Despite this improvement, there still remained the issue that short waves were lost if the ADCP's deployment depth was increased. The solution was to include a vertical beam for Acoustic Surface Tracking (AST), where a direct measure of the distance to the surface could be made and thus estimate surface position [3]. The AST solved the depth limitation for non-directional wave measurements but the limitations for direction waves still remained. This last limitation required addressing the issue of getting the measurement cells (for orbital velocities) closer to

the surface where the signal was less attenuated by depth. In order to accomplish this, a measurement and processing method was developed so that that the ADCP could be mounted on a subsurface buoy and measure waves; one can now imagine a subsurface buoy deployed 30 meters below the surface, and independent of the total water depth. This method is commonly known as the SUV method and really represents a hybrid of the PUV and AST measurements [4].

Alas, it appeared that the limitation for measuring high resolution wave measurements was resolved. Waves from 3-30 seconds could be measured with centimeter accuracy and this was effectively independent of the depth of the water for where the measurements were to be conducted.

The technical challenges for deep water deployments had been solved, but there remained practical limitations. Depths from 0-60 meters can be addressed with a bottom mounted AWAC; greater depths require a subsurface buoy and an AWAC collecting data in SUV mode. The mooring length in this latter configuration has to be a minimum of 60 meters to minimize the effects of buoy motion; additionally the subsurface buoy mounted AWAC should be a safe distance from the surface (20-30 meters). As a result of the minimum mooring length and minimum depth of a subsurface buoy, the minimum total water depth is approximately 80-90 meters for a subsurface mounted AWAC [5]. The result of these requirements led to is that there was a range of depths between 60-80 meters where neither a bottom mounted nor a subsurface buoy mounted AWAC could measure wave directions accurately.

The second weakness of subsurface buoy mounted configuration is that the measurement range of the instrument again was limited to 60 meters. This is fine for short mooring lengths (100-200 meters), but not for moorings that are significantly longer and exposed to currents and drawn down below 60 m.

The 400 kHz AWAC is designed to specifically address the above challenges. The 400 kHz AWAC can be mounted on the bottom for depth up to 100 meters or it may be mounted on a subsurface buoy where the tolerance for mooring draw down is much greater than it would be for a 600 kHz AWAC.

### B. Understanding AST measurement limitations

The Acoustic Surface Tracking (AST) is central in the AWACs wave measurement methods. The estimate of distance to the surface (AST) is free of any complex transfer functions and therefore provides a direct estimate of the surface variations. The AST retains high frequency wave information since it is not lost by attenuation as is the disadvantage with wave related parameters such as velocity and pressure. There are several benefits to this. First, the wave processing is much simpler since there is no complex transfer function to calculate. A direct estimate also means that a time series of the sea surface elevation is available to calculate estimates of  $H_{1/3}$ ,  $H_{1/10}$ ,  $H_{max}$ , and  $T_{mean}$ . Furthermore, it is unaffected by mean currents which impose a Doppler shift on the surface waves - a result requiring special consideration when calculating the frequency dependent transfer function for the velocity and pressure. Perhaps the most important benefit is the simple fact

that wave resolution (shorter wave information) is only mildly affected by increased deployment depth.

Despite all the benefits of the AST, it is not completely without its limitations. The following is a discussion of each of the mechanisms limiting the performance and extends earlier work detailing how the AST operates and its limitations [3].

1) *Speed of sound variations* The distance to the surface is estimated by measuring the two-way travel time of the short pulse transmitted towards the surface together with an estimate of the speed of sound. Deviations between the true speed of sound profile and the estimated profile (here assumed to be uniform with depth) will directly lead to errors in the distance to the surface. The estimated profile is based on a fixed salinity and the measured temperature at the AWAC. These deviations can lead to absolute distance errors of up to 3%, but are typically much less. This presents more of an error for absolute distances than relative distances (such as wave height). The same error applies to the surface excursions, where 3% is an acceptable error for wave heights.

2) *Bubbles* Breaking waves on the surface generate bubbles on the surface which are drawn down in the water column by orbital velocity and turbulence. Bubble clouds can have a relatively broad footprint and persist for as much as 60 seconds. AST performance is affected in two ways. The first is that a pulse will lose energy through scattering as it passes through the bubble cloud on the way to the surface and back to the AWAC, which means that the surface reflection will be weaker. The second point is that it elevates the acoustic noise floor in the vicinity of the returned pulse, making it sometimes difficult to distinguish the surface reflection from bubble clouds. Experience shows that the 600 kHz has a better response than the 1 MHz AWAC, suggesting that it penetrates through the bubble cloud with greater ease. The contour plot in Figure 2 illustrates the extent of bubble clouds. The plot presents the amplitude profile of the AST when the AWAC is operating in a special diagnostic mode.

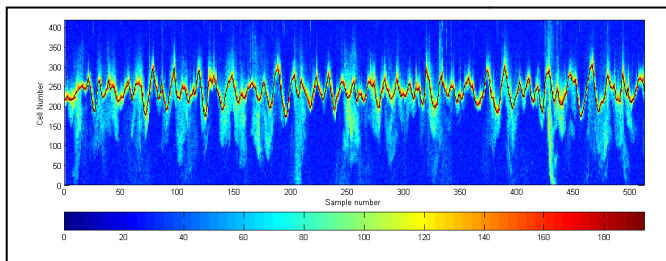


Figure 2. Color contour plot of AST diagnostic data (AST amplitude profile) illustrating aeration of water from breaking waves.

3) *Mounting Angle* Since the acoustic pulse is reflecting from the surface the best response occurs when the pulse path is orthogonal to the surface from which it is reflecting. The return response deteriorates as the beam deviates from vertical. Performance is notably reduced when the tilt exceeds

10 degrees. This also explains why the off-vertical beams for Doppler measurements are not used in this mode.

4) *Footprint* The wave resolution from the AST measurements is not completely independent of deployment depth. There is a mild response, where some high frequency wave information is lost at greater depths. The extent of the high frequency filter is determined by the sea surface area ensonified (sampled) by the AST pulse. The diameter or “footprint” of the ensonified area increases as the distance from the surface increases. When the diameter of this footprint becomes similar in size to a wavelength, then the structure of the waveform (crest and trough) cannot be well resolved. There is an averaging of the distance over the waveform and thus a “smearing” of the true features. A “cut off” frequency is assumed when the footprint diameter is equivalent to half a wavelength. The relationship is plotted in Figure 3, and has been confirmed in field tests [3]

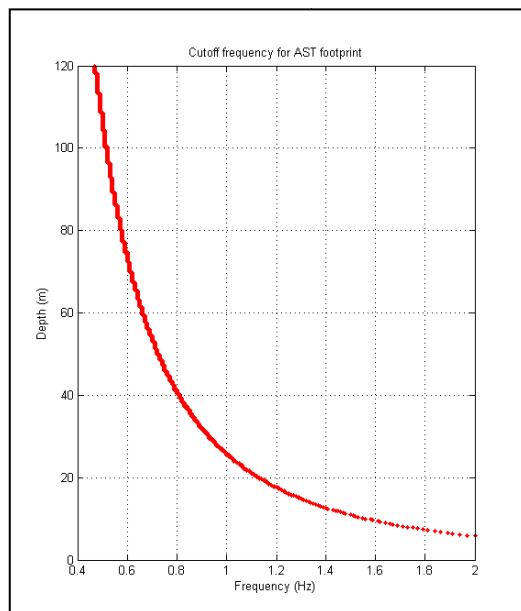


Figure 3. High frequency limitation for AST as a function of depth.

The direct measure of the AST would initial let one believe that it is as simple as opening a window to the surface for a look. The limitations listed show it is not this simple. Fortunately the limitations are quite manageable. A typical deployment will see some ensembles containing multiple false detects. Managing the false detects involves recursively identifying outliers, removing and interpolating between them. It is encouraging that as much as 10% of the time series can have false detects with only a mild effect on the accuracy of  $H_{m0}$ ; moreover this threshold is seldom exceeded.

### C. Understanding measurement limitations - wave direction resolution

Wave directions are estimated by using several measurements of orbital velocity together with the AST. The measurements form an array projected from the AWAC to just

below the surface. The array processing method (Maximum Likelihood Method) exploits the time lags between spatially separated measurements of the array in order to estimate direction. Alternatively the same data may be used in the form of “classic” triplet processing (SUV). The triplet is formed by the AST and two horizontal and orthogonal components of orbital velocity measurements. Both of these directional processing methods rely upon orbital velocity measurements. The frequency dependent response of orbital velocity with depth determines the frequency resolution for wave directions.

Orbital velocities attenuate exponentially with depth and this behavior is more severe for higher frequency waves (short waves). This means that the further down in the water column that the orbital velocities are measured, the less high frequency information is available. This is the classic problem faced by bottom mounted instruments, and note that even the ADCP class of instruments suffers from this challenge if it is not managed effectively.

Managing the response means positioning the measurement cell as close to the surface as possible, while ensuring that there is no contamination from the surface either directly from the cells touching the surface or indirectly from side lobe energy leaking off the main beam. This can be managed by positioning the cells just below the surface by a fraction of the measured depth; 10% of the depth has proven to provide a good signal response without contamination.

It is important to note that the limitation for the directional estimates is also imposed on the non-directional estimates, if orbital velocities are used to estimate the energy density spectrum. An accurate directional estimate is required if the surface wave is to be estimated accurately for each individual beam. This is why the AST remains the primary estimate and the orbital velocity a secondary estimate for energy.

A second limitation imposed on the resolution for directional estimates is associated with the measurements spatial separation. Wave directional estimates become ambiguous when the horizontal separation is equal to half a wavelength. The result is that waves at the associated frequency cannot be accurately estimated. One perceived solution is to position the measurement cells closer to the instrument such that the spatial separation is reduced and consequently the frequency at which this ambiguity occurs is higher. Unfortunately, moving the measurement cell further down in the water column means that the orbital velocity signal disappears. The result is that there is no performance gain by drawing the cells in closer to the instrument.

### III. ICE THICKNESS MEASUREMENTS

#### A. Background

The ability to determine the presence of ice and measure its thickness is becoming more of interest in recent times. This has been partially driven by the oil and gas sector who have found interests at more extreme latitudes where ice adds to the environmental challenges of operations and structure survivability. These measurements are often conducted relatively close to coastal areas where ice keels present the threat of bottom scour to subsea operations and assets. It also becomes interesting during seasonal changes when the ice

begins to break up and blocks of ice are set into motion by waves.

Ice is also of interest for climate modeling. These studies are often associated with more open and deeper water locations. Measurements are performed from subsurface buoys, and ice profiling instruments are positioned further down in the water column to avoid collisions with passing ice keels.

For subsurface instrumentation, the process of estimating ice thickness involves differencing the instrument’s estimates of depth and distance to the water-ice interface. Pressure is used to estimate depth and the AST or echo ranging is used to estimate the distance to the water-ice interface. This method of estimating ice thickness has been in practice for some time now and has been commercially available since the early 1990’s [6][7]. A description of the ice thickness estimate and the sources of error are detailed in the subsequent section discussing uncertainty of ice thickness estimates.

Pressure measurements are usually handled by a high accuracy pressure sensor, where many earlier efforts have employed a Paroscientific pressure sensor [7][8]. The AWAC is now available with its own temperature compensated pressure sensor which has an error of approximately +/-0.1% of full scale or +/-10 cm for 100 meters. In addition to the instruments pressure measurements there needs to be a correction for the atmospheric variations, however this does not seem to be a significant challenge as atmospheric measurements over 100 km away from the deployment site have been used with success [7]. Finally, it should be mentioned that care should be taken when estimating the density, which is used to convert pressure to depth. Previous studies [9] indicate that salinity can vary significantly with depth in coastal areas during the spring thaw.

The distance estimate comes from echo ranging to the water-ice interface and is almost always performed by a vertical oriented acoustic source. Earlier implementations used transmit frequencies ranging from 200 kHz to 400 kHz [6][7]. There have been attempts to use an ADCP for echo ranging, but this involves a considerable amount of effort to correct for error with non-vertical beam orientation [8].

The primary challenge associated with estimating distance from echo ranging is that the distance is directly proportional to the vertically averaged speed of sound estimate. Reasonably accurate estimates of the speed of sound can be made at the instrument’s depth; we know however that the dynamics of the oceans will lead to speed of sound variations (from temperature variations) through the course of the deployment. Measurements of the speed of sound profile are typically not possible because of limited accessibility due to ice.

There are a few techniques however that can be employed to reduce this source of error. The first is to identify “leads” or larger ice free periods and re-calibrate echo ranging estimate. It should be noted that leads in the ice are not always available and often sporadic. Furthermore, the task of identifying an ice free surface is not necessarily a simple task since the scattering characteristics do not lend themselves to use the acoustic return to identify the presence of an opening [7].

It is also possible to reduce the uncertainty of the speed of sound profile by making assumptions about the depth of the mixing layer and how this changes between seasons [8]. It has also been observed that the speed of sound profile experiences little seasonal change below 40 meters in ice prone waters, and therefore a measured profile at the time of deployment and retrieval is valuable in bounding the solution [7].

Another source of error that requires attention is ocean swell from open waters. The pressure signal is significantly attenuated by depth, but the variations at the water-ice interface are detected. This may be handled by filtering techniques, but it does require that the sampling rate is fast enough to remove wave effects [7].

Despite the challenges of addressing all the possible sources of error, the differencing of depth and interface distance is the most attractive means at the present time to identify and estimate dynamic ice draft. A discussion of alternative methods is discussed in [7][9].

### B. Ice Thickness Uncertainty

The magnitude of the thickness tends to be a small fraction of the total depth (an order or two of magnitude), yet it is an absolute error and a function of total depth, and this is why small errors in the depth estimate and interface estimates can lead to relative significant errors in the ice thickness estimate. The following discussion brings to light the sources of error and expected magnitudes.

A simplified version of the ice thickness is the difference between the depths as estimated by the pressure and the distance by the AST estimate from the travel time of the pulse,

$$Depth = \frac{P - P_{Atmos}}{\rho g}, \quad (1)$$

$$Distance = t_0 c, \quad (2)$$

where  $P$  is the measured pressure,  $P_{Atmos}$  is the local atmospheric pressure,  $\rho$  is the water density of sea water,  $g$  is the acceleration of gravity,  $t_0$  is the time it takes for the acoustic signal to reach the water-ice interface and  $c$  is the speed of sound in sea water. The thickness can then be expressed as

$$dZ = \frac{P - P_{Atmos}}{\rho g} - t_0 c. \quad (3)$$

Offset in the absolute pressure,  $P$  can be removed before the ice cover appears by requiring that  $dZ = 0$  when there is no ice. This approach requires that the pressure offset does not change over time, something that usually can be achieved by using a pressure sensor that is temperature compensated.

If the water column density and sound speed is constant and uniform,  $dZ$  is determined only by  $P_{Atmos}$  and  $t_0$ . The atmospheric variations,  $P_{Atmos}$  can vary +/- 0.3 meters, as low and high pressure systems move over the measurement. The parameter is coherent over fairly large horizontal scales and it is often sufficient to get data from a nearby meteorological station. Alternatively, it is possible to filter the pressure measurements over scales of a week or more but this will reduce the time resolution of the ice thickness measurements.

If the temperature of the water column changes over time, the simplified equation (3) is not valid and has to be written with integral form. To first order (assuming small variations in temperature), we can simply replace the density and the speed of sound with their mean equivalents, i.e. the vertically averaged estimates.

$$dZ = \frac{P - P_{Atmos}}{\bar{\rho} g} - t_0 \bar{c}. \quad (4)$$

This implies that the error in  $dZ$  is proportional to the speed of sound and inversely proportional to the density. Since density is inversely proportional to temperature, this means that the two terms are "pulling in the same direction" and ideally one could imagine that the temperature effect cancels out. Unfortunately, the relative variations in the speed of sound are much stronger than the corresponding change in the density (large changes in salinity notwithstanding). As a consequence, the error in ice thickness is dominated by the effect of temperature on the mean speed of sound over the water column.

Figure 4 illustrates the error in the ice thickness from a depth of 100 m assuming that average temperature is in error. The basis for the ice thickness estimate is assumed to be a temperature of 5 degree Celsius, whereas the correct average temperature in the plot is in the interval [-1 to 5] degrees Celsius. The blue line shows the effect on the term (2) and the green line shows the effect on term (1). As it can be seen, the effect of a 6 degree error is quite large; 1.8 meters if the acoustic system is located 100 meters below the surface.

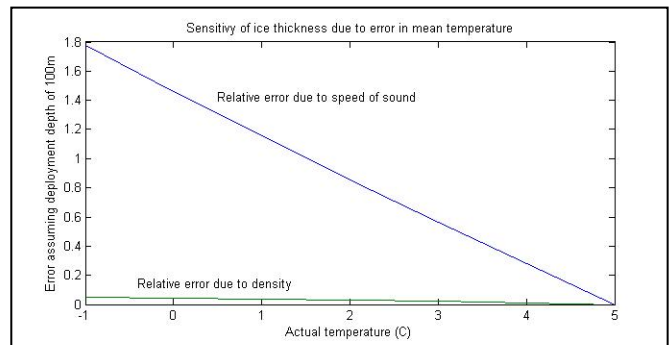


Figure 4. Error estimate for ice thickness, when mean temperature is assumed to be 5 Celius but actual temperature is plotted on horizontal axis. Effects plotted for both error associated with density (green) and speed of sound (blue).

From a practical point of view, an ice thickness measurement system must assume that the depth averaged temperature and hence the speed of sound varies as a continuous function of time. Since temperature measurements are usually only available at the sensor itself, a few tricks can be employed:

- a) If the ice breaks open,  $dZ$  is zero and it is possible to "calibrate" referenced to the pressure. In between these periods, the speed of sound can be interpolated in time.
- b) When ice is forming or is permanently present at the surface, the temperature at the surface can be estimated quite precisely. A first order estimate of the depth average speed of

sound can be found as the mean between the value at the surface and at the instrument.

Overall, it is clear that measurements of absolute ice thickness with acoustic instruments is strongly dependent on the sound speed and that a practical system must take this into account. This is more problematic for fast, stationary ice that does not present the possibility of calibration with occasional, ice-free openings.

There are certainly several challenges in estimating ice thickness which have limited possibilities for improvements with the measurements. It does not mean, however, that nothing can be done to aid the estimation effort.

Identifying ice free periods is an important element of the post processing since the events are both infrequent and important in recalibrating the distance measurements. The task of identifying ice free periods can be improved by using the high sampling rate of the burst mode and process the burst to identify peak energy in the ocean wave band. This could certainly help automating the effort of finding ice free periods and recalibrating the distance measurement and associated mean speed of sound. The wave burst sampling should also aid in identifying false detects from bubble clouds, which has been problematic for early efforts with 400 kHz echo rangers, which did not sample fast enough to identify wave energy [7].

#### IV. DATA

##### A. Ice Data

During the development phase of the ice measurement capability, two 1 MHz AWACs were outfitted with an SD card logger, which provided the capability of recording up to 4 GB of data. Large capacity was in fact useful in the development phase since the AWACs recorded high resolution diagnostic data of the AST return signal strength; resolution was 2.4 centimeters and extended over several meters. The diagnostic AST measurements occurred for every other burst, where burst measurements of 512 samples (1 Hz) were collected every 15 minutes. Clearly a considerable amount of data was to be collected for the yearlong deployment.

There were no direct estimates of the AST distance to water-ice interface. Instead this had to be calculated in post processing. Although there was a considerable amount of data, the diagnostic data did provide the possibility to evaluate different detection methods for the water-ice interface. In the end, a leading edge detection scheme was employed. This high-resolution burst measurement provided information about the mean ice thickness, maximum ice keel draft, and ice block movement.

The project associated with this deployment was to measure ice parameters in support of the design of an offshore structure and its ice armoring. The goals of the project were to measure ice thickness during stationary, fast ice periods and ice block thickness and size distribution during partial ice coverage periods. Two Nortek 1MHz AWAC's with ice measurement

capability were deployed in the Beaufort Sea in August 2008 in about 12 meters water depth and recovered one year later.

An ASL Model IP-5 Ice Profiler was deployed near one of the AWACs for reference ice thickness measurements. The ASL IP-5 uses an upward-looking acoustic echo sounding technique similar to that of the Nortek AWAC, but with a narrower beam and lower acoustic frequency (420 kHz). A comparison of ice thickness during the period of stationary, fast ice shows excellent agreement between the two acoustic measurement methods, with no bias (Fig. 5) and a mean difference of less than 0.05 meters.

Ice formation began in mid-October (Fig. 6) when air temperatures were routinely below -10 degrees C. Following a 3-week period when floating thick blocks of multi-year ice were present, the ice became solid and its keel draft varied only slowly. This suggests that the solid ice was land-fast and consisted of a solid sheet of more-or-less uniform thickness, which is taken to be approximately equal to the ice keel draft and ice thickness, as the density of sea ice is only slightly less than water density. The thickness increased almost linearly until it peaked in mid-May at about 1.8 meters. This represents an increase in ice thickness of approximately 0.01 meter/day. The ice began to thin rapidly in late May and ice breakup occurred in early July, with the breakup and transition to open water lasting only a few days.

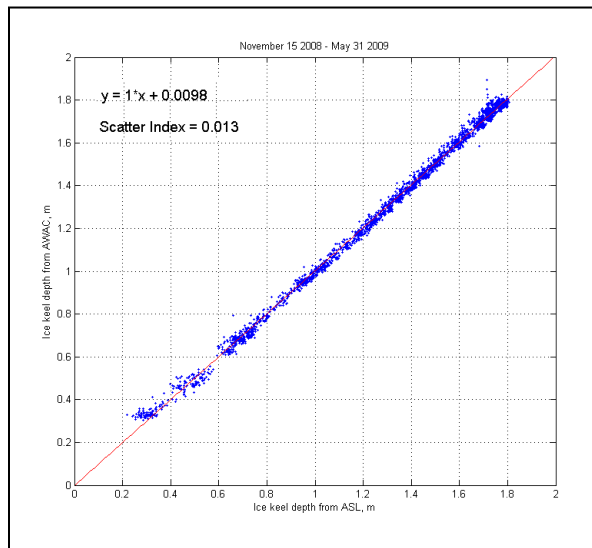


Figure 5. Comparison of ice thickness estimates for Nortek AWAC and ASL Ice Profiler.

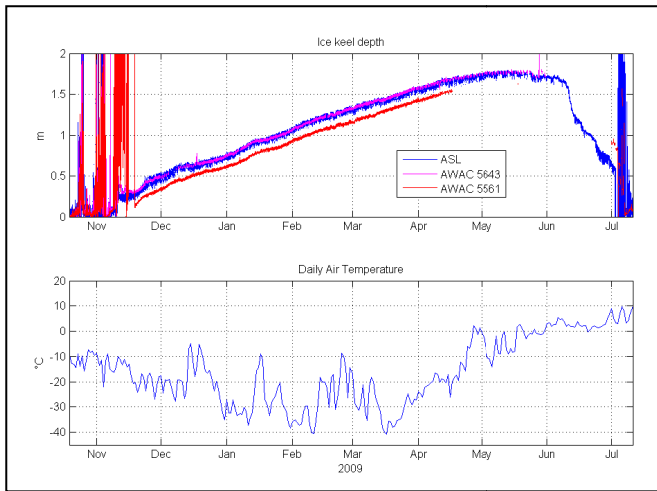


Figure 6. Ice thickness from two AWACs and one ASL Ice Profiler (top). The ASL and AWAC 5643 were deployed in the same bottom frame, while AWAC 5561 was deployed about 2 km away in slightly different water depth. Daily air temperature (bottom).

### B. 400 kHz AWAC Wave Data

The performance of the 400 kHz AWAC wave measurements were evaluated by comparing to a 600 kHz AWAC. The 600 kHz AWAC was deployed at a shallower depth and therefore expected to provide higher frequency resolution. The 400 kHz AWAC was deployed at 90 meters depth and the 600 kHz AWAC was deployed at 19 meters depth. This deployment location is near Færder, which is to the south of Oslo fjord where the fjord opens into the North Sea (Figure 7). The location is relatively protected but occasionally experiences long wave energy (e.g., longer than 8 seconds). The location also has a persistent southerly current which can range from 0.5-1.0 m/s and typically is opposing the wave direction.

Since the AWAC's AST and directional processing have been independently validated on several previous occasions, the main intention of the test was to evaluate the depth response for both the AST and directional processing. The test design is not well suited for a rigorous comparison for several reasons. This includes the fact that (a) the deployment length was only 10 days, (b) the reference instrument was deployed several hundred meters away and at a different depth, (c) ensemble (burst) measurements were offset by 30 minutes. Nonetheless, the test served its purpose of providing an indication of how the said methods performed at 90 meters depth.

The AST proved to perform remarkably well and there did not seem to be any deviation from what could have been expected. The test period of 10 days provided 240 wave bursts, where each burst contained 2048 samples. Most bursts had no false detects and the maximum number of false detects was 3 samples in a single wave burst. The frequency resolution associated with the ensonified footprint on the surface was consistent with the estimates from the AST beam width and range. This is illustrated in Figure 8 where a 24 hour period of energy density spectra have been averaged together; this was

done for both the 400 and 600 kHz AWACs. The high frequency limit is indicated by where the energy density spectra begins to level off, and thus represents where the footprint size begins to extend over a greater portion of a single wavelength. You will note that this is not a discrete change, but a gradual effect. This seems to become significant at approximately 0.5 Hz which is consistent with the model presented in Figure 3.

It is also interesting to note that there is a low frequency noise floor for the wave measurements, which is approximately an order of magnitude greater for the 400 kHz AWAC, than that witnessed by the 600 kHz AWAC at 19 meters depth. One possible explanation for the perceived low frequency energy is that there are greater fluctuations of the speed of sound (i.e., temperature) as different masses pass over the AWAC during the wave burst measurement. These fluctuations manifest themselves as variations in the overall range, albeit small relative to the surface wave variations.

The 400 kHz AWAC's estimates of significant wave height ( $H_{m0}$ ) and peak period ( $T_{peak}$ ) show good agreement with that of the nearby 600 kHz AWAC (Fig. 9). Peak Periods are as short as 2 seconds and the wave heights as little as 30 cm. The directional estimates show a greater variability and not quite as good agreement. There is a notable difference in the first and second half of the deployment. The first half shows a consistent direction from the south-southwest, whereas the second half is noted by random estimates. The reason for this is that the peak period shortens from 8 seconds to less than 4 seconds. When it reaches 4 seconds, the orbital velocities at depth are no longer measurable. Here we witness the frequency limit for directional estimate at approximately 4 seconds for a deployment depth of 90 meters. The two AWACs have an apparent bias of the wave directions for the first half of the deployment; the most plausible explanation is refraction that occurs between the spatially separated AWACs.

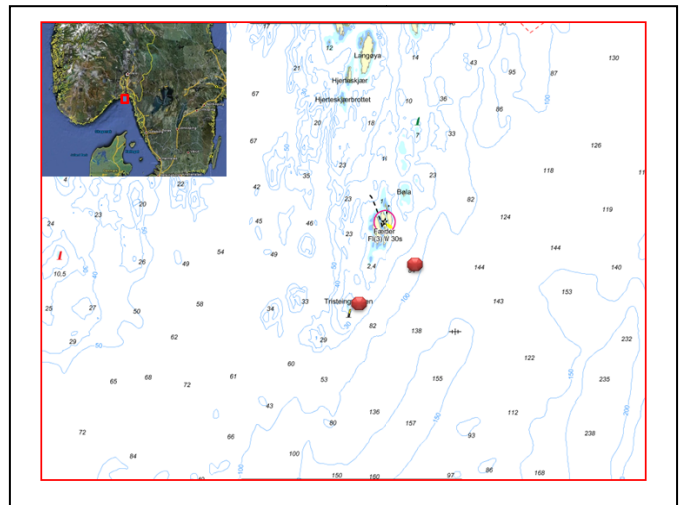


Figure 7. Chart with depths showing the 600 kHz AWAC (lower red circle) and the 400 kHz (upper red circle) deployment location. Insert is the regional map showing the deployment location (red box), relative to Norway, Sweden and Denmark.

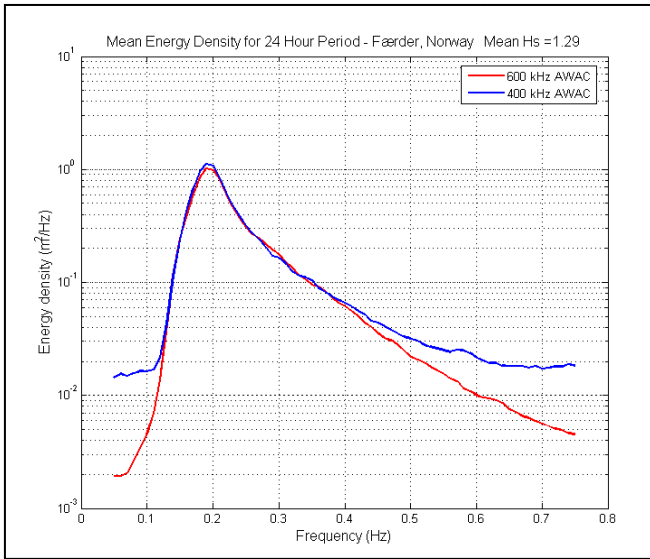


Figure 8. Energy density spectra averaged over 24 hours. Blue is the 400 kHz AWAC, red is the 600 kHz AWAC.

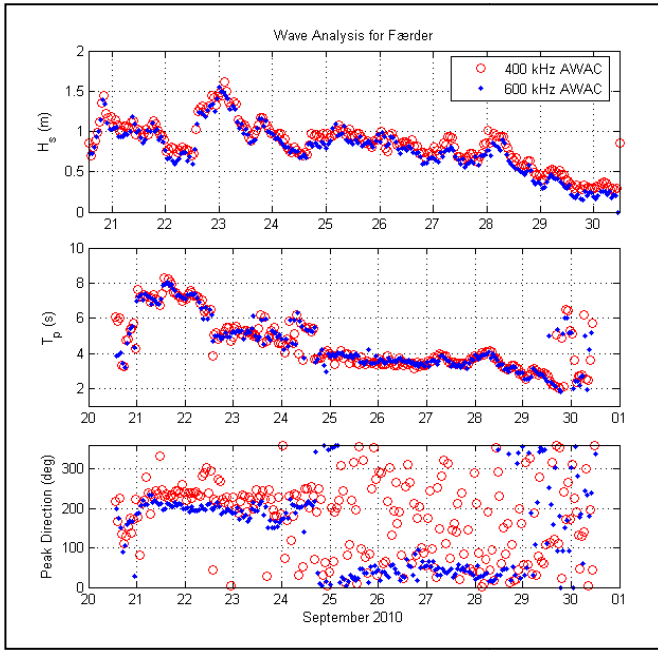


Figure 9. Wave estimates of  $H_{m0}$ ,  $T_{peak}$ , Peak Direction for the 400 kHz AWAC (red) and the 600 kHz AWAC (blue).

## V. CONCLUSIONS

A new deep water version of the AWAC is introduced. It is intended to measure high resolution wave data despite the challenges associated with subsurface wave measurement instruments. The 400 kHz AWAC is similar in operation to the 1 MHz and 600 kHz AWACs, but differs in that it transmits on two frequencies, 400 kHz for Doppler measurements and 600 kHz for AST measurements. The dual frequencies are selected in order to achieve current profiling over 100 meter range, while maintaining the narrow beam width for the AST.

The intention of this new AWAC is to expand the measurement capabilities to include distance to water-ice interface. A new temperature compensated pressure sensor and firmware designed to measure waves and ice in the same wave burst allows for seasonal data of waves and ice. This is done without having to modify the configuration or change modes.

The error analysis presented indicates that unknown variations in the speed of sound profile is the largest source of error for ice thickness measurements. Thickness errors can exceed 1.0 meter for deployment depths of 100 meters. The art of the problem is to model the speed of sound profile by using assumptions of the behavior and structure of the profile over depth and time. This effort benefits by measuring the profile of the speed of sound at deployment and retrieval time; it is also of benefit to recalibrate the estimated mean speed of sound when open water presents itself – leads in the ice.

Comparison data for ice thickness measurements is provided courtesy of Woods Hole Group, which was collected in the Beaufort Sea, Alaska. The comparison between a 1 MHz AWAC and an ASL ice profiler agree very well, with a bias error of 0.05 meters. This suggests that the AST measurements are well suited for ice measurements.

A review of wave resolution limits are presented for the directional and AST measurements. Understanding these limits becomes important when deployment depths approach 100 meters. Initial tests of the 400 kHz AWAC (compared to a nearby 600 kHz AWAC) confirm our understanding of the limits. Furthermore the comparison test shows that the 400 kHz AWAC can measure peak periods as short as 2 seconds and wave heights as low as 30 cm for a deployment depth of 90 meters. Directional estimates illustrate the low frequency cutoff, which occurs at approximately 0.25 Hz (4 second peak period); this is an encouraging result considering the deployment depth. A more rigorous evaluation remains, where another reference instrument can be collocated, so that similar wave directions can be compared.

## ACKNOWLEDGMENT

The authors would like to thank Bruce Magnell and Leonid Ivanov of Woods Hole Group for the contribution of the ice data.

## REFERENCES

- [1] Grosskopf, W.G., Aubrey, D.G., Mattie, M.G., Mathiesen, M., "Field intercomparison of nearshore directional wave sensors", *IEEE Journal of Oceanic Engineering*, Vol. OE8, No. 4, October 1983.
- [2] Krogstad, H.E., Miller, M.C. and Gordon, R.L., "High-resolution directional wave spectra from horizontally mounted acoustic Doppler current meters", *J. Atmos. Ocean. Technology.*, Vol. 5, no. 4, pp.340-352, 1988.
- [3] Pedersen, T., and Lohrmann, A., "Possibilities and limitations of acoustic surface tracking", *Proceedings Oceans 2004*, Kobe, Japan, 2004.
- [4] Pedersen, T., Lohrmann, A., and Krogstad, H.E., "Wave measurements from a subsurface platform", *Proceedings WAVES 2005*, Madrid, Spain, 2005.
- [5] Pedersen, T., and Siegel, E., "Wave measurements for subsurface buoys", *Proceedings Current Measurement Technology Conference IEEE*, Charleston, S.C., 2008
- [6] Melling, H., Johnston, P.H., Riedel, D.A., "Measurements of the underside topography of sea ice by moored subsea sonar", *J. Atmos. Oceanic Technology*, pp. 589-602, June 1995.
- [7] Melling, H., "Sound scattering from sea ice: Aspects relevant to ice-draft profiling by sonar", *J. Atmos. Oceanic Technology*, August 1998, pp.1023-1034.
- [8] Shcherbina, A.Y., Rudnick, D.L., Talley, L.D., "Ice-draft profiling from bottom-mounted ADCP Data", *J. Atmos. Oceanic Technology*, August 2005, pp.1249-1266.
- [9] B. Magnell, L. Ivanov, E. Siegel, "Measurements of ice parameters in the Beaufort Sea using the Nortek AWAC acoustic Doppler current profiler", *Proceedings Oceans 2010*.